Order versus disorder in the quantum Heisenberg antiferromagnet on the *kagomé* lattice using exact spectra analysis

P. Lecheminant
Groupe de Physique Statistique, Université de Cergy-Pontoise, site de Saint-Martin, 2 avenue Adolphe Chauvin, 95302 Cergy-Pontoise Cedex, France

B. Bernu and C. Lhuillier
Laboratoire de Physique Théorique des Liquides, URA 765 of CNRS, Université P. et M. Curie, Boîte Postale 121, 4 Place Jussieu, 75252 Paris Cedex, France

L. Pierre
Université Paris-X, Nanterre, 92001 Nanterre Cedex, France

P. Sindzingre
Laboratorie de Physique Théorique des Liquides, URA 765 of CNRS, Université P. et M. Curie, Boîte Postale 121, 4 Place Jussieu, 75252 Paris Cedex, France

(Received 7 April 1997)

A group-symmetry analysis of the low-lying levels of the spin-1/2 *kagomé* Heisenberg antiferromagnet is performed for small samples up to $N=27$. This approach allows one to follow the effect of quantum fluctuations when the sample size increases. The results contradict the scenario of ''order by disorder'' which has been advanced on the basis of large-S calculations. A large enough second-neighbor ferromagnetic exchange coupling is needed to stabilize the $\sqrt{3}\times\sqrt{3}$ pattern: the finite-size analysis indicates a quantum critical transition at a nonzero coupling. [S0163-1829(97)05229-6]

I. INTRODUCTION

There are very few simple two-dimensional magnets which fail to order at $T=0$. There is now a large amount of evidence that the $S=1/2$ nearest-neighbor Heisenberg antiferromagnet is ordered not only on the square lattice[1] but also on the triangular lattice (TAH).[2–9] The reduction of the order parameter by quantum fluctuations is about 40% for the square lattice and of the order of 50% for the triangular lattice: frustration indeed enhances the role of the quantum fluctuations but the relatively high coordination number plays against them. The *kagomé* lattice which can be seen as a diluted triangular lattice (see Fig. 1) exhibits both frustration and low coordinance number and the $S=1/2$ Heisenberg antiferromagnet on the *kagomé* (KAH) is a good candidate for a disordered two-dimensional quantum liquid.

Exact diagonalizations on periodic samples have shown that the spin-spin correlations decrease indeed very rapidly with distance.[10–12] Series expansion from the Ising limit and high-temperature series point to the absence of magnetic order.[13,14] Large-N approaches, using Sp(N) bosons,[15] find a disordered ground state with unbroken symmetry for small enough spin while, using SU(N) fermions, a spin-Peierls phase or a chiral phase is suggested.[16] The best variational energies for the $N=36$ sample are built from the short-ranged dimerized basis.[17]

On the other hand, semiclassical approaches[18–22] plead in favor of a magnetic order (the $\sqrt{3}\times\sqrt{3}$ state, see Fig. 1) induced by quantum fluctuations (''order by disorder.''[23]) This kind of phenomenon has already been seen in much simpler situations where there is a classical degeneracy between two kinds of orders.[24,25] The J_1-J_2 model on the triangular lattice for large enough J_2 ($J_2/J_1>1/8$) possesses classically degenerate ordered ground states with, respectively, two and four sublattices.[26] Large spin calculations have predicted that quantum fluctuations should select the two sublattices order.[27,28] The study of small samples spectra has confirmed this prediction and shown the mechanism of this selection.[29]

The *kagomé* antiferromagnet is a more problematic issue because of the infinite number of classically degenerate ground states.[30,31] The linear spin-wave approach for the *kagomé* antiferromagnet does not lift the extensive degeneracy of the classical ground state (at this order the spectrum of magnetic excitations possesses a whole branch of zero modes.[18,30,31]) One has to invoke nonlinear processes to stabilize the $\sqrt{3}\times\sqrt{3}$ ordered solution.[19,20,22] On the other hand, one should note that in this class of problem there exist some situations where the ''order by disorder'' phenomenon fails for systems with a ground-state manifold associated with an extensive entropy. An example is the quantum Heisenberg antiferromagnet on the triangular Husimi cactus[32] where the system prefers to remain a spin liquid rather than localizing in a particular ordered state that breaks the degeneracy of the classical ground-state manifold. Moreover, the possibility of a quantum tunneling between different classical states might prevent the system from localizing in a particular ordered solution.[33,34]

This paper is a scrutiny of the conjecture of selection of order by quantum fluctuations based on the study of the low-lying levels of exact spectra. The paper is organized as fol-

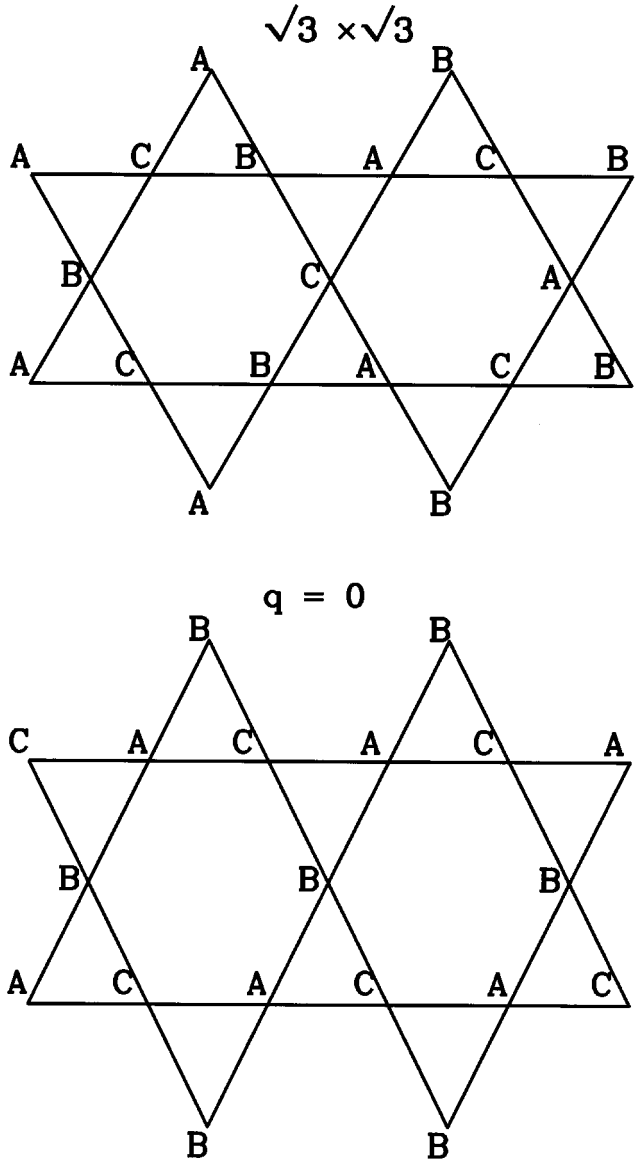

FIG. 1. Two classical planar states of the KAH: the $\sqrt{3}\times\sqrt{3}$ and $\mathbf{q}=\mathbf{0}$ states.

lows: A brief presentation of our method to investigate the finite-size properties of an ordered antiferromagnet is given in the next section. In Sec. III, we apply this method to the search of the selection of the $\sqrt{3}\times\sqrt{3}$ state by quantum fluctuations. In Sec. IV, we introduce a second-neighbor ferromagnetic exchange coupling ($J_2<0$) and show that for large enough $|J_2|$, the system orders through the $\sqrt{3}\times\sqrt{3}$ state. The rigidity of the KAH and the hypothesis of an incommensurable planar order are investigated in Sec. V. Section VI, finally, summarizes our results and lists some open questions.

II. REVIEW OF THE METHOD

The presence of order in a quantum antiferromagnet is readily seen by examination of the low lying levels of its spectrum. The method used in this work has been described in detail in Refs. 4, 7 and 29. We give here a summary of its most important features. The first characteristic of an ordered antiferromagnet (classical or quantum) is the existence of ferromagnetic sublattices: the total spin of each ferromagnetic sublattice is the collective variable relevant for the description of the low-energy spectrum of the system. On a finite lattice with p sublattices of Q sites (the total number of sites being $N=pQ$), the p identical spins $Q/2$ couple to form the rotationally invariant states that are the low-lying eigenstates of the Hamiltonian. These p coupled spins form a ''generalized top'' which precesses freely: elementary mechanics (confirmed by the nonlinear σ model approach[35–37]) indicates that the leading term of this precession is

$$H_{\text{eff}}=\frac{\mathbf{S}^2}{2I_N}. \tag{1}$$

In an ordered system, I_N, the inertia of the top is an extensive quantity, proportional to the perpendicular susceptiblity of the magnet.[4,37] In a disordered system with a gap this quantity is asymptotically constant, and at the quantum critical point between the two regimes I_N is expected to vary as $N^{-1/2}$.[37] The coupling of the $pQ/2$ spins gives $N_S(N,S,p)$ states for each S value of the total spin of the sample and a total of $(Q+1)^p$ levels obeying the effective dynamics of Eq. (1). These levels form the quantum counterpart of the classical ground state: they represent the tower of states indicated by Anderson in his 1952 famous paper.[38] In our spectral representation where the eigenstate energies are displayed as a function of $S(S+1)$ in order to exhibit the free precession [Eq. (1)], the tower is in fact a ''Pisa tower'' with a slope decreasing with the sample size. In the thermodynamic limit, all these low-lying levels (called QDJS in Ref. 4 for quasidegenerate joint states) collapse to the absolute ground state as N^{-1}. An experimental proof of these levels has recently been reported in the analysis of macroscopic quantum coherence in antiferromagnets.[39] It could be noticed that in the thermodynamic limit these levels give a ground-state entropy proportional to $\ln(N^p)$. Above these first family of levels, the spectrum of an ordered antiferromagnet exhibits the magnon spectrum; the low-lying levels of this part of the spectrum collapse more slowly than the QDJS to the ground state with a scaling law $N^{-1/2}$. Three features of the Pisa tower of QDJS are thus essential:

(i) the overall effective dynamics of a finite family of levels (of the order of N^p) and its finite-size scaling leading to a clear cut separation from the first inhomogeneous magnon excitations (the absence of separation between the scaling laws would sign a quantum critical behavior[37]).

(ii) the numbers of levels $N_S(N,S,p)$ in each S subset which for given N and S is determined by the number p of ferromagnetic sublattices of the underlying Néel order,

(iii) the spatial symmetries of these $N_S(N,S,p)$ levels: The number and nature of the space group irreducible representations (SGIR) that appear in each S subspace are uniquely determined by the geometrical symmetries of the Néel order.

The exact diagonalization of the Heisenberg Hamiltonian on small samples enables us to examine these features and to determine the nature of the ordering. This approach has been used for the quantum Heisenberg antiferromagnet on the triangular lattice[4,7] and the J_1-J_2 problem on the triangular lattice.[29]

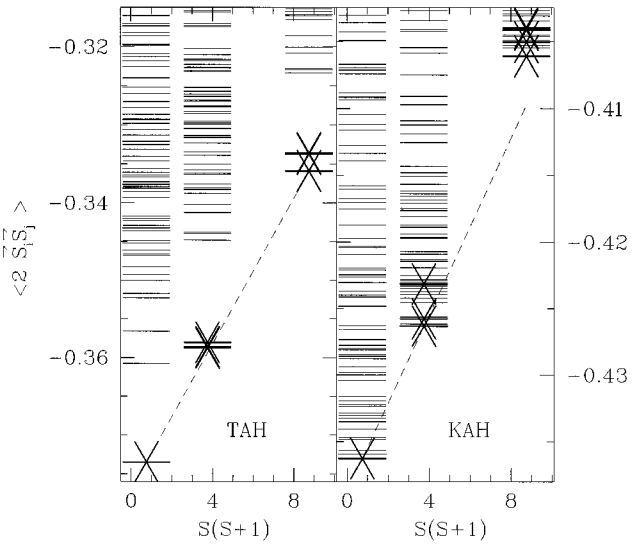

FIG. 2. The low-lying energy levels of the TAH and KAH spectrum of the $N=27$ sample. The levels which possess the symmetry expected for an ordered solution are denoted by a star. The Pisa tower of the TAH is easily seen, quite distinct from the first-magnon excitations. In the KAH, on the contrary, the levels candidate for the building of a tower of states are mixed with other representations in a continuum of excitations.

III. THE LOW-LYING LEVELS OF THE KAH

The Hamiltonian of the KAH, including further-neighbor interactions, has the form

$$\mathcal{H}=2J_1\sum_{\langle i,j\rangle}\mathbf{S}_i\cdot\mathbf{S}_j+2J_2\sum_{\langle\langle i,k\rangle\rangle}\mathbf{S}_i\cdot\mathbf{S}_k, \tag{2}$$

where the $\mathbf{S}_i$ are spin-1/2 quantum operators on the sites of the *kagomé* lattice and $\langle i,j\rangle$ (respectively $\langle\langle i,k\rangle\rangle$) denotes a sum over first (respectively, second) neighbors. In this section, we shall only consider first-neighbor exchange interactions ($J_2=0$). At first sight, the spectrum of the KAH has one feature which is common to all the Heisenberg antiferromagnet spectra that we have been studying: the absolute ground state has a total spin $S=0$ or 1/2 depending on the number of sites of the sample ($N=9,12,15,18,21,24,27$) and the ground-state energy $E_0(S)$ of the S sectors order with increasing S values. Lieb and Mattis[40] have shown that this result is exact for bipartite lattices: our numerical results tend to indicate an extremely robust property (the theorem seems to be true for the Heisenberg antiferromagnet on the triangular and *kagomé* lattices and for the J_1-J_2 problem: none of these situations can be reduced to a bipartite problem). Taken apart from this feature the spectra of the KAH appear totally different from the spectra of the TAH. In Fig. 2, the low-lying levels of the TAH and of the KAH are shown for the 27 site samples:

(i) whereas the Pisa tower is easily seen on the TAH spectrum, well separated from the magnons spectrum, there is absolutely no such scale in the KAH one,

(ii) the effective dynamics of the low-lying levels of the KAH spectrum do not scale as $S(S+1)$,

(iii) the symmetries of the lowest lying levels of each S subspace do not allow the description of an ordered structure: for $N=27$, all the SGIR, but one, appear in the low-lying doublet states below the first $S=3/2$ eigenstates, whereas their number N_S and nature are strictly determined in the case of an ordered solution.

One could argue that the proliferation of these low-lying levels are the quantum counterpart of the infinite degeneracy of the classical ground state with respect to local spin rotations. The real question is: do the quantum fluctuations show any trend to select a specific Néel order?

We have looked to this question for the so-called $\mathbf{q}=\mathbf{0}$ order, the $\sqrt{3}\times\sqrt{3}$ order and for any planar order (see Sec. V). The $\mathbf{q}=\mathbf{0}$ order is studied in Ref. 41. We give here the details of the analysis concerning the $\sqrt{3}\times\sqrt{3}$ order, which is the favored solution found in the semiclassical approaches.[18–22] The smallest lattices where periodic boundary conditions are compatible with this order are $N=9$, 27, and 36 sites. In this section, we shall consider explicitly the $N=27$ sample since the $N=9$ sites is too small and the $N=36$ sample is too large to compute all the levels in each S sector. The QDJS associated with the $\sqrt{3}\times\sqrt{3}$ state are homogeneous on each ferromagnetic sublattice (their wave vectors are either $\mathbf{k}=\mathbf{0}$ or $\mathbf{k}=\pm\mathbf{k_0}$: corners of the Brillouin zone). They do not break the C_{3v} symmetry of the lattice. The three irreducible representations (IR's) characterizing the $\sqrt{3}\times\sqrt{3}$ order are the following:

$$\begin{cases}\Gamma_1:\ [\mathbf{k}=\mathbf{0},\mathcal{R}_\pi\Psi=\Psi,\mathcal{R}_{2\pi/3}\Psi=\Psi,\sigma_x\Psi=\Psi]\\ \Gamma_2:\ [\mathbf{k}=\mathbf{0},\mathcal{R}_\pi\Psi=-\Psi,\mathcal{R}_{2\pi/3}\Psi=\Psi,\sigma_x\Psi=\Psi]\\ \Gamma_3:\ [\mathbf{k}=\pm\mathbf{k}_0,\mathcal{R}_{2\pi/3}\Psi=\Psi,\sigma_x\Psi=\Psi],\end{cases} \tag{3}$$

where $\mathcal{R}_\phi$ is a rotation of angle ϕ and σ_x denotes an axial symmetry. The numbers $N_S(N,S,p=3)$ of levels in the Pisa tower for each value of the total spin are given by the coupling of three $N/6$ spins:

$$\mathcal{D}^{N/6}\otimes\mathcal{D}^{N/6}\otimes\mathcal{D}^{N/6}=\sum_{S=0}^{N/6}(2S+1)\mathcal{D}^S+\sum_{S=N/6+1}^{N/2}(N/2-S+1)\mathcal{D}^S, \tag{4}$$

where $\mathcal{D}^S$ denotes the irreducible representation for a spin S. Therefore, one obtains the numbers $N_S(N,S,p=3)$:

$$N_S(N,S,p=3)=(2S+1)\min(2S+1,N/2-S+1). \tag{5}$$

We notice that in each S sector, an ordered solution contains a number of levels which is strictly related to the number of sublattices of the selected order: in the lower S subspace this number is independent of the sample size for $p\leqslant 3$ [it is the Hilbert space dimension of a rotator or a symmetric top for $p=2$ (respectively, $p=3$)]. In each S subspace, amongst the $N_S(N,S,p=3)$ levels, the number of appearance ($n_{\Gamma_i}^{(S)}$) of the Γ_i IR can be computed following Refs. 7 and 29:

$$n_{\Gamma_i}^{(S)}=\frac{1}{6}\sum_k \mathrm{Tr}(R_k|_S)\chi_i(k)N_{\mathrm{el}}(k), \tag{6}$$

where the summation index k runs through the classes of the S_3 group (isomorphic to C_{3v}); $\chi_i(k)$, $N_{\mathrm{el}}(k)$ denotes, respectively, the characters of the Γ_i IR and the number of ele-

TABLE I. Character table of the permutation group S_3. The first line indicates classes of permutations. The number of elements in each class is $N_{\rm el}$.

S_3	I	(A,B,C)	(A,B)
$N_{\rm el}$	1	2	3
Γ_1	1	1	1
Γ_2	1	1	-1
Γ_3	2	-1	0

ments in the class k (see Table I). The traces of the permutations of S_3 in the S subspace, denoted $\mathrm{Tr}(R_k|_S)$, are determined as

$$\mathrm{Tr}(R_k|_S)=\mathrm{Tr}(R_k|_{S_z=S})-\mathrm{Tr}(R_k|_{S_z=S+1}), \tag{7}$$

and

$$\begin{cases} \mathrm{Tr}(I_d|_{S_z})=\displaystyle\sum_{t,v,x=-N/6}^{N/6}\delta_{t+v+x,S_z} \\ \mathrm{Tr}((A,B)|_{S_z})=\displaystyle\sum_{t,v=-N/6}^{N/6}\delta_{2t+v,S_z} \\ \mathrm{Tr}((A,B,C)|_{S_z})=\displaystyle\sum_{t=-N/6}^{N/6}\delta_{3t,S_z}, \end{cases} \tag{8}$$

where (A,B) [respectively (A,B,C)] stands for a two-body (respectively, three-body) permutation of S_3. The final results of the computation of the $n_{\Gamma_i}^{(S)}$ are given for the $N=27$ sample in Table II.

The lowest levels in the first S subspaces of the $N=27$ sample spectrum are given in Table III. The levels which have the good symmetries to describe a $\sqrt{3}\times\sqrt{3}$ antiferromagnet are displayed with an asterisk: most of these $N_S(N=27,S,p=3)$ levels are rather far in the spectrum and many levels belonging to other SGIR proliferate between them. In fact, in the odd N samples, the number of low-lying $S=1/2$ states below the first $S=3/2$ states increases very rapidly with the system size, the trend seems the same in the even samples (see Fig. 3). Altogether these numbers of low-lying levels grow seemingly roughly as α^N with $\alpha\simeq 1.18$ (respectively, $\alpha\simeq 1.14$) in the odd (respectively, even) samples. Note that these numbers lay between the ground-state degeneracy of the three-states Potts model[42] ($\alpha\simeq 1.134$) and the degeneracy of the Dimer model[43] ($\alpha=2^{1/3}\simeq 1.26$). This exponential proliferation of low-lying levels with all spatial symmetries is certainly the deepest proof of the absence of long-range antiferromagnetic order: it signs both the absence of a finite number of ordered sublattices (that is the absence of an antiferromagnetic order parameter) and the impossibility of a Néel symmetry breaking.

The selection of order by quantum fluctuations previously observed in the J_1-J_2 model on a triangular lattice is quite different.[29] In that last model the four-sublattice QDJS family is perfectly pure on the smallest nonfrustrating sample spectra: the two-sublattice QDJS family is a subset of the first family. Quantum fluctuations just stabilize this subset relatively to the entire four-sublattice family and thus build a

TABLE II. Number of occurrences $n_{\Gamma_i}^{(S)}$ of each irreducible representation Γ_i $(i=1,2,3)$ with respect to the total spin S.

$N=27$														
$2S$	1	3	5	7	9	11	13	15	17	19	21	23	25	27
$n_{\Gamma_1}^{(S)}$	0	1	1	1	2	2	1	2	1	1	1	1	0	1
$n_{\Gamma_2}^{(S)}$	0	1	1	1	2	1	1	1	1	0	1	0	0	0
$n_{\Gamma_3}^{(S)}$	1	1	2	3	3	3	3	2	2	2	1	1	1	0

TABLE III. Lowest eigenenergies (with degeneracy and quantum numbers) of the $N=27$ sample spectrum. Components of **k** are in units $6\pi/N$. In the three last columns, 1 stands for invariant under the symmetry, 0 for no symmetry, and -1 for a nontrivial phase factor under the above mentioned symmetry (i.e., $e^{i2\pi/3}$ for the rotation of $2\pi/3$ and -1 for the two others). Stars indicate states possessing the symmetries associated with the $\sqrt{3}\times\sqrt{3}$ state. The double horizontal bar indicates the omission of 127 $S=1/2$ states before the first levels in the $S=3/2$ subspace.

$N=27$	$\langle 2\mathbf{S}_i\cdot\mathbf{S}_j\rangle$	$2S$	Deg.	**k**		$\mathcal{R}_{2\pi/3}$	$\mathcal{R}_{\pi}$	σ_x
	-0.43627796	1	4	0	0	-1	1	0
	*-0.43627796	1	4	3	6	1	0	1
	-0.43622206	1	12	0	3	0	0	-1
	-0.43593382	1	12	0	3	0	0	1
	-0.43591527	1	8	3	6	-1	0	0
	-0.43563229	1	12	0	3	0	0	1
	-0.42632327	3	8	0	0	-1	1	0
	*-0.42632327	3	8	3	6	1	0	1
	-0.42630998	1	8	3	6	-1	0	0
	-0.42615931	3	16	3	6	-1	0	0
	*-0.42577308	3	4	0	0	1	1	1
	-0.42562690	3	8	0	0	-1	1	0
	-0.42562690	3	8	3	6	1	0	1
	-0.42485791	1	8	3	6	-1	0	0
	-0.42483901	1	4	0	0	-1	1	0
	-0.42483901	1	4	3	6	1	0	1
	-0.42479279	1	4	0	0	-1	-1	0
	-0.42479279	1	4	3	6	1	0	-1
	-0.42455077	3	24	0	3	0	0	1
	-0.42419453	3	16	3	6	-1	0	0
	-0.42419310	3	4	0	0	1	1	1
	-0.42417083	1	2	0	0	1	1	1
	-0.42405358	1	2	0	0	1	1	-1
	-0.42405358	1	2	0	0	1	-1	1
	-0.42394796	1	8	3	6	-1	0	0
	-0.42391172	3	24	0	3	0	0	1
	-0.42372061	3	24	0	3	0	0	-1
	-0.42366979	1	2	0	0	1	1	1
	-0.42347751	3	4	0	0	1	-1	-1
	-0.42333145	3	24	0	3	0	0	-1
	-0.42324731	3	8	0	0	-1	1	0
	-0.42324731	3	8	3	6	1	0	1
	-0.42318668	3	24	0	3	0	0	-1
	*-0.42314189	3	4	0	0	1	-1	1
	-0.42314189	3	4	0	0	1	1	-1

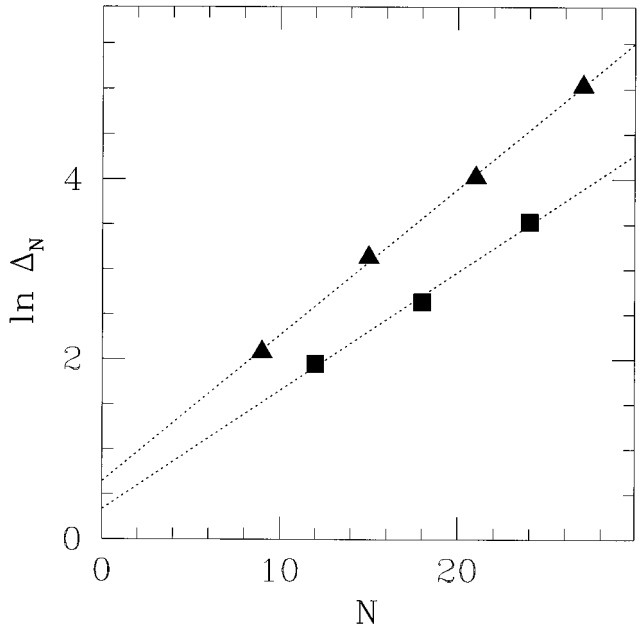

FIG. 3. Logarithm of the number Δ_N of $S=1/2$ levels below the first $S=3/2$ level as a function of the sample size N (black triangles). This number, which does not take into account the twofold magnetic degeneracy, is compared to the same quantity (square symbols) for the even N samples (i.e., number of $S=0$ levels below the first $S=1$ level).

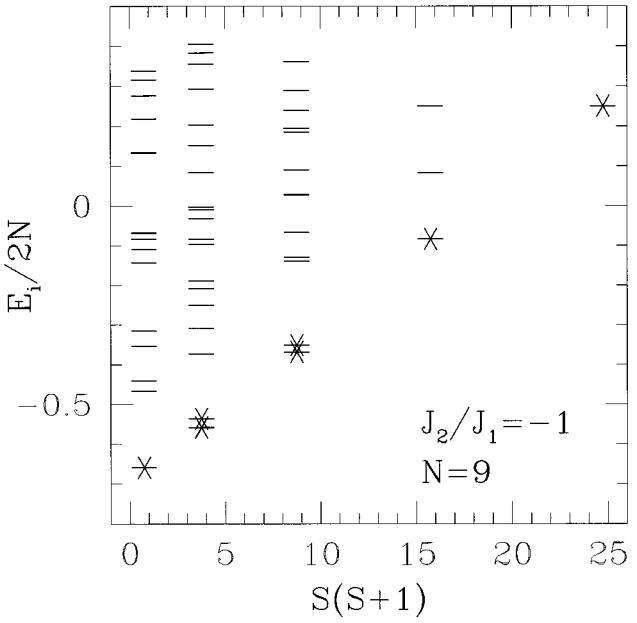

FIG. 4. Low-lying spectrum of the $N=9$ sample with $|J_2|/J_1=1$ and periodic boundary conditions, as a function of $S(S+1)$. Note the Pisa tower associated with the $\sqrt{3}\times\sqrt{3}$ state.

simpler structure with an order parameter of higher symmetry: They do not create the order parameter, but just renormalize it and increase its intrinsic symmetry.

IV. ORDERING WITH A SECOND-NEIGHBOR FERROMAGNETIC EXCHANGE COUPLING

In order to ascertain our conclusion and reinforce the credibility of the method, we have studied with the same protocol the problem of the *kagomé* lattice with a first-neighbor antiferromagnetic interaction J_1 and a second neighbor ferromagnetic interaction J_2 [see Eq. (2)] favoring the existence of a $\sqrt{3}\times\sqrt{3}$ order. For large enough $J_2<0$, the spectrum has all the expected features of a Pisa tower of QDJS (dynamics, number of states, and symmetries) associated with this order (see Fig. 4 for the $N=9$ sample). When $|J_2|/J_1$ decreases the Pisa tower disappears, indicating the existence of a quantum phase transition. The estimate of the critical value of J_2/J_1 is a difficult task requiring a study of finite-size effects. The smallest sizes compatible with the $\sqrt{3}\times\sqrt{3}$ order are $N=9,27,36$ sites: computing time and memory requirements for such an extensive study remain prohibitive. However, using appropriate twisted boundary conditions ($\pm 2\pi/3$ around the z axis, see Ref. 7 and the Appendix), we can use the intermediate $N=12,21$ samples. The twisted boundary conditions break the rotational spin symmetry of the Hamiltonian and fix the Néel plane perpendicular to the twist axis. The helicity of Néel order is thus fixed along the z axis and the free dynamics of the system reduces to the precession of the total spin around z. The effective Hamiltonian reads:

$$\mathcal{H}_{\text{eff}}=\frac{S_z^2}{2I_3}, \tag{9}$$

where I_3 is the inertia of the top along the z axis. The degeneracy of each S_z^2 subspace is 2 ($\pm S_z$). The IR characterizing the $\sqrt{3}\times\sqrt{3}$ order is Γ_1: [$\mathbf{k}=\mathbf{0}, \mathcal{R}_{2\pi/3}\Psi=\Psi$, $\sigma_x\Psi=\Psi$]. Figure 5 shows the tower of states associated with the $\sqrt{3}\times\sqrt{3}$ order for the $N=21$ sample with $|J_2/J_1|=1$.

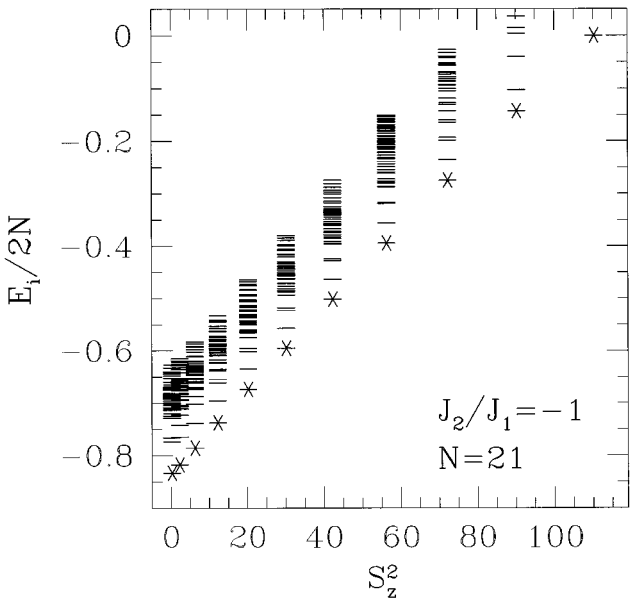

FIG. 5. Low-lying spectrum of the $N=21$ sample with $|J_2|/J_1=1$ as a function of S_z^2. A twist of $2\pi/3$ in the boundary conditions is applied to accomodate the $\sqrt{3}\times\sqrt{3}$ state with the sample size. Due to the boundary conditions, the Pisa tower reduces to one IR for each S_z value.

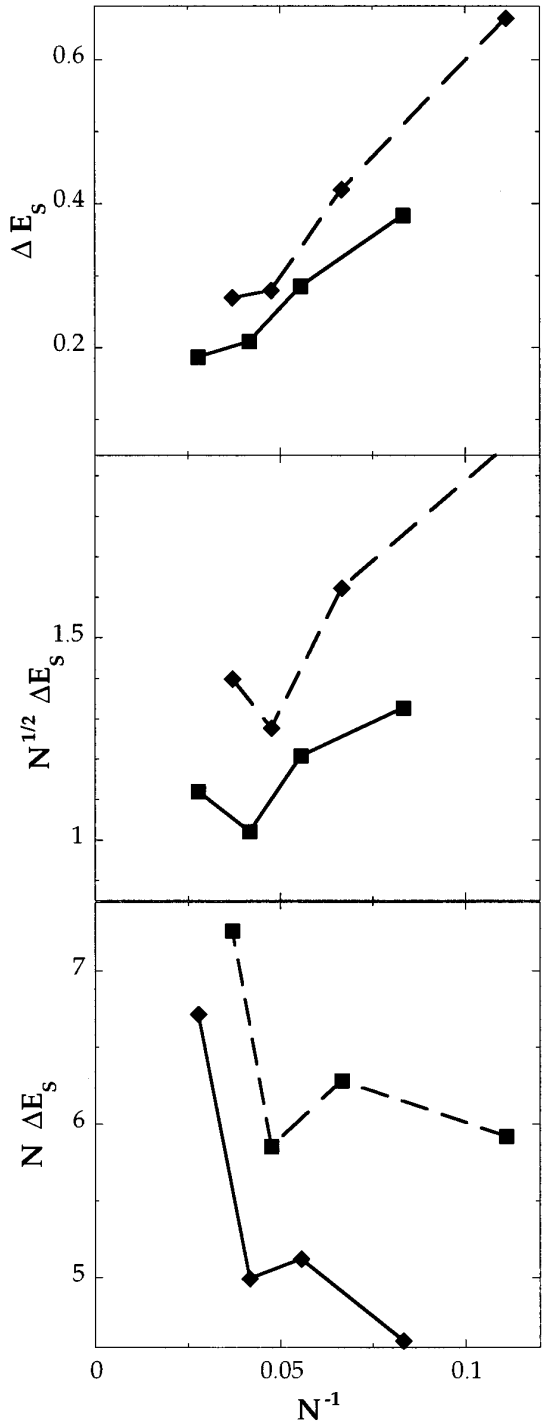

FIG. 6. Finite-size study of the ''spin gap'' $\Delta E_s = E_0(S_{z,\min}+1) - E_0(S_{z,\min})$ of the pure KAH ($J_2=0$) as a function of the sample size. This energy is $\mathcal{O}(N^{\alpha})$ with $\alpha=-1, -1/2$, or 0 whether the system is ordered, critical or disordered. Continuous lines (respectively, broken lines) are guides for the eye through the even N (respectively, odd N) results. The comparison of the three quantities ΔE_s, $N^{1/2}\times\Delta E_s$, and $N\times\Delta E_s$ versus N^{-1} favors the hypothesis of spin disorder.

The order parameter or the spin stiffness of these levels scale as $N^{-1/2}$, whereas the slope of the Pisa tower scales as N^{-2}. At first sight, it seems thus more efficient to use this information to look at the transition between order and disorder as $|J_2|/J_1$ is decreased. This can be done in a rather

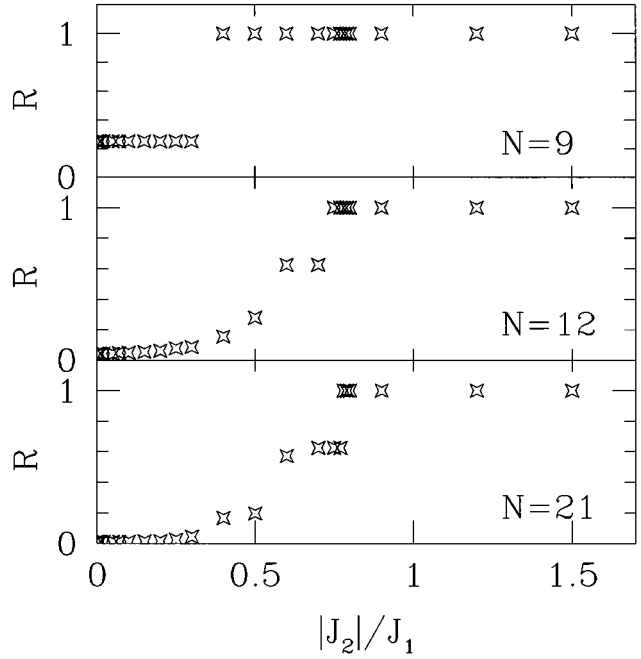

FIG. 7. Behavior of the ''index of order'' (R) as a function of $|J_2|/J_1$ and of the system size.

naive way by looking at the spin gap between the ground state of $S_{z,\min}$ and $S_{z,\min}+1$: in the ordered phase this quantity should scale as N^{-1} (respectively, $N^{-1/2}$ and N^0 in the critical and disordered phase): this study is done in Fig. 6 for the case $|J_2/J_1|=0$ (pure KAH). It shows, thanks to the trends in the larger sample sizes, that the KAH is certainly not ordered, probably not critical but truly disordered.

This naive use of the Pisa tower does not account for the whole qualitative information contained in the QDJS family which is described both by the effective Hamiltonian and by the space-group symmetry of the levels. This information is incorporated in the index R measuring the ''degree of order'' present in the low lying levels, and defined as follows:

(i) First, we consider the ordered phase (with $|J_2/J_1|\geqslant 1$) and concentrate on all the low-lying levels of the Pisa tower that are lower in energy than the softest magnons: for each sample size this determines the number of S_z sectors which give a consistent picture of the ''quasiclassical ground state.'' Precisely we search for the lower level of the spectrum with a nonzero wave vector in the magnetic Brillouin zone $[E_{\min}(\mathbf{k})]$ and determine $S_{z,\max}$ as the largest value of S_z such that $E_0[S_{z,\max}+1]\leqslant E_{\min}(\mathbf{k})$. By definition $E_0(S_{z,\max}+1)$ is thus smaller than the energy of the softest magnon of the sample and in the thermodynamic limit $S_{z,\max}$ grows roughly as $N^{1/4}$.

(ii) In each S_z subspace considering all the levels in the energy range $[E_0(S_z),E_0(S_z+1)]$ we define r_{S_z} as the ratio of the number of levels compatible with $\sqrt{3}\times\sqrt{3}$ order to the total number of levels of this range (r_{S_z} is a number between 0 and 1).

(iii) We then compute the index R measuring the degree of order of the sample as the average of the ratios r_{S_z} for S_z running from 0 (respectively, 1/2) up to $S_{z,\max}$.

This index is equal to one if the lowest levels form a true Pisa tower and decreases when other IR's appear in the low-

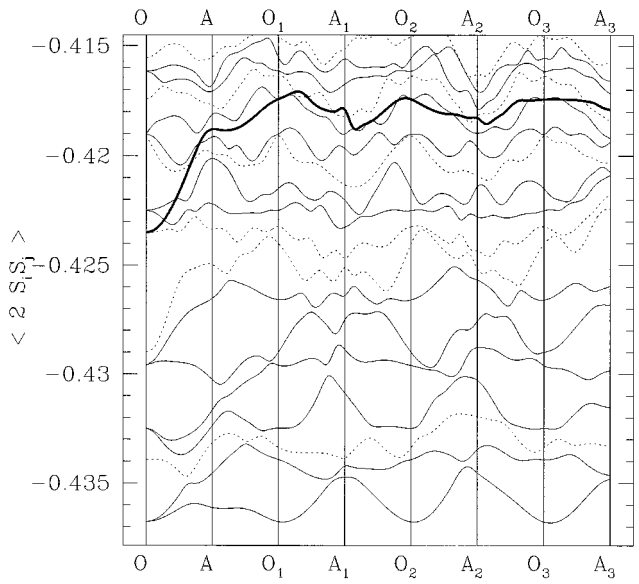

FIG. 8. Variation of the energy per link $\langle 2\mathbf{S}_i\cdot\mathbf{S}_j\rangle$ of the low-lying levels of the $N=21$ sample versus twisted boundary conditions Φ_1 ($\Phi_2=0$). O_i are the points where $\Phi_1=0$ (mod 2π). O_7 is the first point where the twist per link is 0 (mod 2π). The points A_k [$\Phi_1=\pi$ (mod 2π)] are in the middle of O_i and O_{i+1}. Because the figure is symmetric with respect to A_3, the part A_3-O_7 is not represented here. Note that most of the levels do not come back to their original assignation after a 2π twist of the boundary conditions. In fact on this small size sample, due to an extra symmetry when $\Phi_i=0$, the uniform $\mathbf{k}=\mathbf{0}$ ground state is degenerate with the first star of $\mathbf{k}\neq\mathbf{0}$ eigenstates. Only the $\mathbf{k}=\mathbf{0}$ states and their continuation have been shown in OA_1. The six other $\mathbf{k}\neq\mathbf{0}$ in OA are found by folding the O_iA_i onto OA. Full lines stand for states going continuously to $\mathbf{k}=\mathbf{0}$ chiral states (complex IR's of C_3), dashed lines stand for states going continuously to the first star of $\mathbf{k}\neq\mathbf{0}$ eigenstates, the $\mathbf{k}=\mathbf{0}$ nonchiral states (trivial IR of C_3); bold line: the first $S_z=3/2$ level.

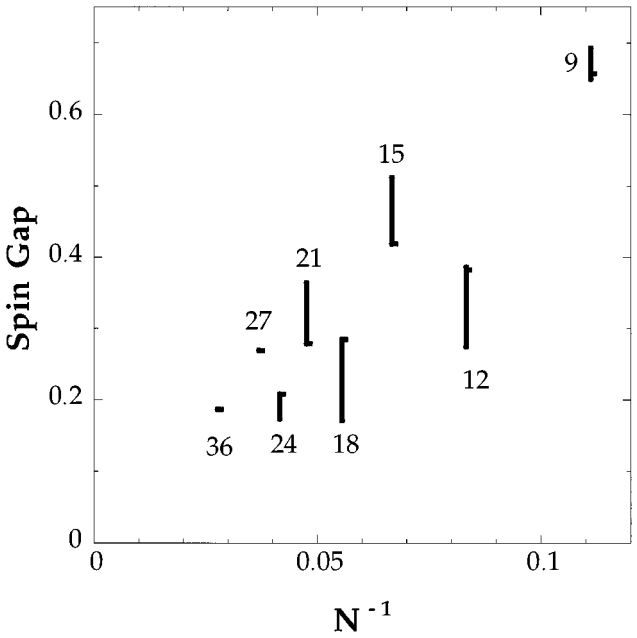

FIG. 9. Variations of the ''spin gap'' with boundary conditions: the small horizontal tick gives the value of the gap for periodic boundary conditions. There is a systematic effect: the $\Delta S=1$ excitation energy decreases with the twists of the boundary conditions in the even N samples and increases in the odd N ones.

lying levels of the spectrum when $|J_2/J_1|$ is decreased. R is thus a measure of the breakdown of order which includes qualitative information on the low-lying levels. It stands on the quantities that scale more rapidly with the system size.

The variations of this index as a function of $|J_2|/J_1$ and of the sample size are given in Fig. 7. When $|J_2/J_1|=0$ this index goes very rapidly to zero with N: this supports the idea that the KAH is indeed disordered and that quantum fluctuations show no tendency to select ''order from disorder'' in the disordered phase. More unexpected, the finite-size scaling on R indicates that a small ferromagnetic exchange is not sufficient to establish long-range order in the system and that the value of the critical ratio $(|J_2|/J_1)_c$ is probably larger than 0.5.

V. INCOMMENSURATE MAGNETIC ORDER

The previous study discards the hypothesis of a $\sqrt{3}\times\sqrt{3}$ order in the pure KAH (we did the same check with the same conclusion for the $\mathbf{q}=\mathbf{0}$ order in Ref. 41). Using twisted boundary conditions $\mathbf{S}_{\mathbf{r}_i+\mathbf{T}_{\alpha=1,2}}=\mathcal{R}_{\mathbf{z}}(\Phi_{\alpha=1,2})\mathbf{S}_{\mathbf{r}_i}$ across the sample defined by the vectors $\mathbf{T}_{\alpha=1,2}$ (see the Appendix for more details), we have extended our search to any planar antiferromagnetically ordered configurations, either commensurate or incommensurate. The existence of a planar order, if any, would be signed by a minimum of the ground-state energy for a given pair of twist angles (Φ_1,Φ_2) and the appearance of a Pisa tower for these parameters.[7] A typical result of a set of diagonalizations is shown in Fig. 8 for the $N=21$ sample. Sweeping the Brillouin zone for (Φ_1,Φ_2), we have studied in this way the spectra of the $N=9,12,15,18,21,24,27$ samples. We observe the following properties:

(i) The influence of the twisted boundary conditions is very small, much smaller than for the TAH: on the $N=21$ sample the effect of the twist on the ground state of the KAH is only 8% of the same effect on the TAH. This is coherent with the picture of a disordered, liquid system.

(ii) We do not find a signature of any planar antiferromagnetic order for any size. Very shallow minima appear in the spectra, but they are never associated with a tower of QDJS and the position of these minima changes from place to place with the sample size.

(iii) The ''spin gap'' between the ground-state energy of the $S_z=0$ (or 1/2) subspace and the ground-state energy of the S_z+1 subspace $[\Delta E_s=E_0(S_z+1)-E_0(S_z)]$ has only small variations with the twists (Fig. 9). These variations appear systematic, and show a different trend in the even and odd samples: this could be related to the fact that the odd samples only accomodate spin-1/2 excitations of the thermodynamic absolute ground state which is a true singlet. (This hypothesis is examined in a companion paper.[44])

VI. CONCLUSION

Using the analysis of the low-lying levels of the Heisenberg antiferromagnet on a *kagomé* lattice we have shown evidence that the system has no planar antiferromagnetic

long-range order at $T=0$. Introducing a small second-neighbor ferromagnetic exchange coupling does not seem to be sufficient to establish long-range order: from the experimental point of view this is good news as it could perhaps enlarge the number of candidates for a spin-liquid behavior.

The theoretical study of the tower of low-lying levels (Pisa tower) that we have developed in this paper seems potentially useful to give an approximate location of the transition from order to disorder even on small samples: its advantage over other approaches stands on the finite-size scaling of the parameter we are looking at and on the inclusion in this parameter of qualitative information on the macroscopic ground state.

According to our present results, this spin-1/2 model exhibits a quantum critical point at a nonzero $|J_2|/J_1$. It would be interesting to investigate the universality class of this quantum critical point and see how it may compare to the theoretical predictions of the nonlinear σ model for canted antiferromagnets.[45]

ACKNOWLEDGMENTS

We have benefited from a grant of computer time at Center de Calcul Vectoriel pour la Recherche (CCVR), Palaiseau, France.

APPENDIX: TWISTED BOUNDARY CONDITIONS

For a sample defined by the two vectors:

$$\begin{cases} \mathbf{T}_1 = 2(l+m)\mathbf{u}_1 + 2m\mathbf{u}_2 \\ \mathbf{T}_2 = 2l\mathbf{u}_1 + 2(l+m)\mathbf{u}_2, \end{cases} \tag{A1}$$

where $\mathbf{u}_1$ and $\mathbf{u}_2$ are two unit vectors of the *kagomé* lattice, and m and n are two integers related to the number of sites of the sample by $N=3(l^2+m^2+lm)$, the boundary conditions are defined through

$$\mathbf{S}_{\mathbf{r}_i+\mathbf{T}_{\alpha=1,2}} = \mathcal{R}_{\mathbf{z}}(\Phi_{\alpha=1,2})\mathbf{S}_{\mathbf{r}_i}, \tag{A2}$$

where $\mathbf{r}_i$ denotes the sites of the *kagomé* lattice. In order to recover the translation invariance that seems to be broken by these boundary conditions, the spin frame at the point $\mathbf{r}_i+\mathbf{u}_1$ (respectively, $\mathbf{r}_i+\mathbf{u}_2$) is rotated with respect to the spin frame at point $\mathbf{r}_i$ by an angle θ_1 (respectively, θ_2). The boundary angles $\Phi_{\alpha=1,2}$ are related to $\theta_{\alpha=1,2}$ by the relations

$$\begin{cases} \Phi_1 = 2(l+m)\theta_1 + 2m\theta_2 \\ \Phi_2 = 2l\theta_1 + 2(l+m)\theta_2. \end{cases} \tag{A3}$$

The Hamiltonian in the new frame reads

$$\mathcal{H} = 2J_1 \sum_{\substack{i=1,N \\ \mu=1,3}} \tilde{\mathbf{S}}_{\mathbf{r}_i} . \mathcal{R}_z(\theta_\mu) \tilde{\mathbf{S}}_{\mathbf{r}_i+\mathbf{u}_\mu}. \tag{A4}$$

θ_1 and θ_2 are changed step by step so that Φ_1 and Φ_2 sweep the appropriate fraction of the Brillouin zone of this problem.

[1] E. Manousakis, Rev. Mod. Phys. **63**, 1 (1991), see references therein.
[2] D. A. Huse and V. Elser, Phys. Rev. Lett. **60**, 2531 (1988).
[3] T. Jolicoeur and J. C. Le Guillou, Phys. Rev. B **40**, 2727 (1989).
[4] B. Bernu, C. Lhuillier, and L. Pierre, Phys. Rev. Lett. **69**, 2590 (1992).
[5] R. Deutscher and H. U. Everts, Z. Phys. B **93**, 77 (1993).
[6] N. Elstner, R. R. P. Singh, and A. P. Young, Phys. Rev. Lett. **71**, 1629 (1993).
[7] B. Bernu, P. Lecheminant, C. Lhuillier, and L. Pierre, Phys. Rev. B **50**, 10 048 (1994).
[8] P. Lecheminant, B. Bernu, C. Lhuillier, and L. Pierre, Phys. Rev. B **52**, 9162 (1995).
[9] M. Boninsegni, Phys. Rev. B **52**, 15 304 (1995).
[10] C. Zeng and V. Elser, Phys. Rev. B **42**, 8436 (1990).
[11] J. T. Chalker and J. F. G. Eastmond, Phys. Rev. B **46**, 14 201 (1992).
[12] P. W. Leung and V. Elser, Phys. Rev. B **47**, 5459 (1993).
[13] R. R. P. Singh and D. A. Huse, Phys. Rev. Lett. **68**, 1766 (1992).
[14] N. Elstner and A. P. Young, Phys. Rev. B **50**, 6871 (1994).
[15] S. Sachdev, Phys. Rev. B **45**, 12 377 (1992).
[16] J. B. Marston and C. Zeng, J. Appl. Phys. **69**, 5962 (1991).
[17] C. Zeng and V. Elser, Phys. Rev. B **51**, 8318 (1995).
[18] A. B. Harris, C. Kallin, and A. J. Berlinsky, Phys. Rev. B **45**, 2899 (1992).
[19] A. Chubukov, Phys. Rev. Lett. **69**, 832 (1992).
[20] A. Chubukov, J. Appl. Phys. **73**, 5639 (1993).
[21] L. O. Manuel, A. E. Trumper, C. J. Gazza, and H. A. Ceccatto, Phys. Rev. B **50**, 1313 (1994).
[22] H. Asakawa and M. Suzuki, Int. J. Mod. Phys. B **9**, 933 (1995).
[23] J. Villain, R. Bidaux, J.-P. Carton, and R. Conte, J. Phys. (France) **41**, 1263 (1980).
[24] E. F. Shender, Sov. Phys. JETP **56**, 178 (1982).
[25] C. L. Henley, Phys. Rev. Lett. **62**, 2056 (1989).
[26] T. Jolicoeur, E. Dagotto, E. Gagliano, and S. Bacci, Phys. Rev. B **42**, 4800 (1990).
[27] A. Chubukov and T. Jolicoeur, Phys. Rev. B **46**, 11 137 (1992).
[28] S. E. Korshunov, Phys. Rev. B **47**, 6165 (1993).
[29] P. Lecheminant, B. Bernu, C. Lhuillier, and L. Pierre, Phys. Rev. B **52**, 6647 (1995).
[30] J. T. Chalker, P. C. W. Holdsworth, and E. F. Shender, Phys. Rev. Lett. **68**, 855 (1992).
[31] P. Chandra, P. Coleman, and I. Ritchey, J. Phys. (France) I **3**, 591 (1993).
[32] P. Chandra and B. Doucot, J. Phys. A **27**, 1541 (1994).
[33] J. von Delft and C. L. Henley, Phys. Rev. Lett. **69**, 3236 (1992).
[34] J. von Delft and C. L. Henley, Phys. Rev. B **48**, 965 (1993).
[35] D. S. Fisher, Phys. Rev. B **39**, 11 783 (1989).
[36] H. Neuberger and T. Ziman, Phys. Rev. B **39**, 2608 (1989).
[37] P. Azaria, B. Delamotte, and D. Mouhanna, Phys. Rev. Lett. **70**, 2483 (1993).

[38] P. W. Anderson, Phys. Rev. **86**, 694 (1952).
[39] G. Levine and J. Howard, Phys. Rev. Lett. **75**, 4142 (1995).
[40] E. Lieb and D. Mattis, J. Math. Phys. (N.Y.) **3**, 749 (1962).
[41] P. Lecheminant, Ph.D. thesis, Université Pierre et Marie Curie, Paris, 1995.
[42] R. J. Baxter, J. Math. Phys. (N.Y.) **11**, 784 (1970).
[43] V. Elser, Phys. Rev. Lett. **62**, 2405 (1989).
[44] B. Bernu, P. Lecheminant, C. Lhuillier, L. Pierre, and P. Sindzingre, Phys. Rev. Lett. (to be published).
[45] P. Azaria, B. Delamotte, and D. Mouhanna, Phys. Rev. Lett. **68**, 1762 (1992); A. Chubukov, T. Senthil, and S. Sachdev, *ibid.* **72**, 2089 (1994); A. Chubukov, S. Sachdev, and T. Senthil, Nucl. Phys. **B426**, 601 (1994).